STAR Protocols

CellPress
OPEN ACCESS

Protocol

Stratifying ferroptosis sensitivity in cells and mouse tissues by photochemical activation of lipid peroxidation and fluorescent imaging

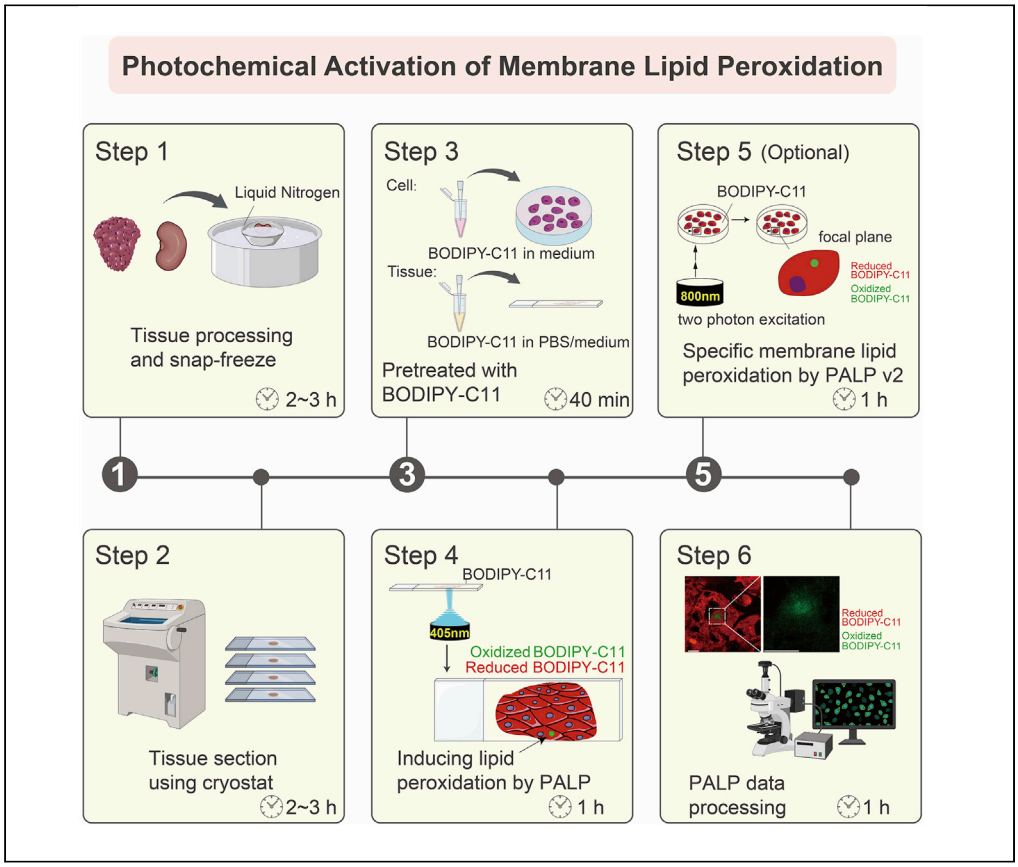

Ferroptosis is a non-apoptotic iron-dependent cell death. Here we present a protocol for stratifying ferroptosis sensitivity in cells and mouse tissues. This protocol uses photochemical activation of lipid peroxidation (PALP) coupled with fluorescent imaging to assess the relative sensitivity to ferroptosis. Using commercial reagents and common equipment, PALP is readily accessible to most laboratories. One remaining challenge is the inability to multiplex this technique in analyzing multiple tissues or regions simultaneously. This protocol may have applications in developing ferroptosis-targeted therapies.

Fengxiang Wang, Nathchar Naowarojna, Yilong Zou

wangfengxiang@westlake.edu.cn (F.W.)
zouyilong@westlake.edu.cn (Y.Z.)

Highlights

Protocol for photochemical activation of membrane lipid peroxidation

Estimation of sensitivity to ferroptosis in live cell and tissue *in situ*

Enabling study of lipid peroxidation on specific cellular membrane

Wang et al., STAR Protocols 3, 101189
June 17, 2022
https://doi.org/10.1016/j.xpro.2022.101189

STAR Protocols

CellPress
OPEN ACCESS

Protocol

Stratifying ferroptosis sensitivity in cells and mouse tissues by photochemical activation of lipid peroxidation and fluorescent imaging

Fengxiang Wang,[1,2,3,4,5,*] Nathchar Naowarojna,[2,3,4] and Yilong Zou[2,3,4,6,*]

[1]College of Life Sciences, Zhejiang University, Hangzhou, Zhejiang 310058 China

[2]Westlake Four-Dimensional Dynamic Metabolomics (Meta4D) Lab, Westlake Laboratory of Life Sciences and Biomedicine, Hangzhou, Zhejiang 310024 China

[3]School of Life Sciences, Westlake University, Hangzhou, Zhejiang 310024 China

[4]Westlake Institute for Advanced Study, Hangzhou, Zhejiang 310024 China

[5]Technical contact

[6]Lead contact

*Correspondence: wangfengxiang@westlake.edu.cn (F.W.), zouyilong@westlake.edu.cn (Y.Z.)
https://doi.org/10.1016/j.xpro.2022.101189

SUMMARY

Ferroptosis is a non-apoptotic iron-dependent cell death. Here we present a protocol for stratifying ferroptosis sensitivity in cells and mouse tissues. This protocol uses photochemical activation of lipid peroxidation (PALP) coupled with fluorescent imaging to assess the relative sensitivity to ferroptosis. Using commercial reagents and common equipment, PALP is readily accessible to most laboratories. One remaining challenge is the inability to multiplex this technique in analyzing multiple tissues or regions simultaneously. This protocol may have applications in developing ferroptosis-targeted therapies.

For complete details on the use and execution of this protocol, please refer to Wang et al. (2021).

BEFORE YOU BEGIN

Ferroptosis is a non-apoptotic, iron-dependent form of oxidative cell death characterized by uncontrolled peroxidation of polyunsaturated fatty acid (PUFA)-containing phospholipids. Ferroptosis induction has been implicated as a new therapeutic strategy for treating various cancers (Jiang et al., 2021). However, rapidly stratifying cells or cancer patients for their sensitivity to ferroptosis induction remains a major challenge in developing ferroptosis-targeted anti-cancer treatment (Jiang et al., 2021). Herein, we establish a technique termed photochemical activation of membrane lipid peroxidation (PALP) to detect polyunsaturated phospholipids as well as report ferroptosis sensitivity in live cells and tissues *in situ*.

This protocol provides a detailed description of the PALP technique aimed to stratify ferroptosis sensitivity in cells and tissues *in situ*. Essential materials for this method include: fresh cell and tissue samples, cryostat for tissue sectioning, confocal microscope/spinning-disk confocal microscope/multi-photon microscope or equivalent, BODIPY™ 581/591 C11 (fluorescent reporter for lipid peroxidation), and imaging analysis software. Before implementing this protocol, users need to be familiar with the principle/usage of confocal microscopes and tissue sectioning procedures. While this protocol focuses on using PALP to analyze cancer cells in culture and tissues dissected from mouse models, this technique can, in principle, be applied to any cultured cells and fresh tissue samples.

For tumor tissue in this protocol, we subcutaneously injected one group of female athymic nude mice (5 weeks old, 18–20 g, n=3) with 2×10^6 human OVCAR-8 cells on the left flank and with

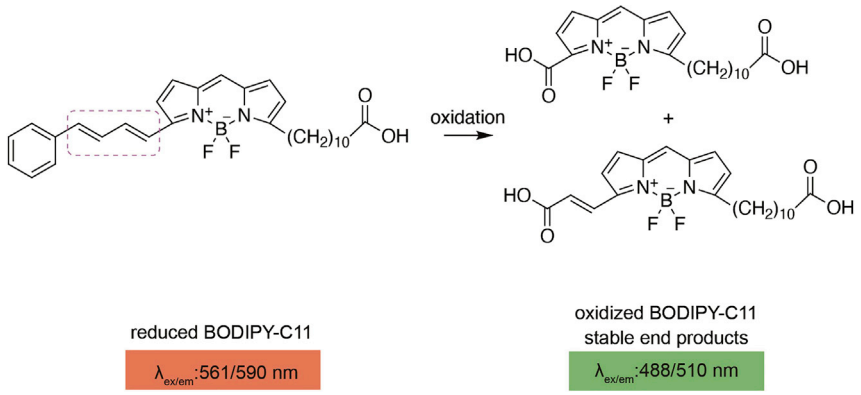

Figure 1. Oxidative reaction of BODIPY-C11 581/591 probe by PALP application, related to before you begin

1×10^6 ES-2 cells on the right flank. Another group of mice from same lineage(n=3) were subcutaneously injected with 1×10^6 OV56 cells on the left flank and with 1×10^6 SKOV3 cells on the right flank. The mice were sacrificed when the tumor volume reached ~ 60 mm^3. Animal experiments were carried out in accordance with the animal protocol approved by the Institutional Animal Care and Use Committee (IACUC) of Westlake University.

Preparation of fluorescent lipid peroxidation reporter reagent

Timing: 10 min

This protocol uses BODIPY™ 581/591 C11 (Life Technologies, D3861) as the reporter for lipid peroxidation. BODIPY-C11 can be used to detect reactive oxygen species (ROS) in lipophilic environments such as cellular membranes. Oxidation of the polyunsaturated butadienyl structure in BODIPY-C11 results in a shift of fluorescence emission peak from ~590 nm to ~510 nm (Figure 1) (Drummen et al., 2002). We recommend preparing BODIPY-C11 at 5 mM (1000×) stock concentration with the working concentration of 5 μM (1×). In principle, other fluorescent reporters of lipid peroxidation could be used in place of BODIPY-C11.

BODIPY™ 581/591 C11 stock solution (1000×)		
Reagent	Final concentration	Amount
BODIPY C11	5 mM	1 mg
DMSO	n/a	0.4 mL
Total	**5 mM**	**0.4 mL**

⚠ CRITICAL: Keep the stock solution in −20°C shielded from light and aliquot in small portions to avoid freeze-thaw cycles for more than twice. The maximum storage time is one year.

BODIPY™ 581/591 C11 working solution (1×)		
Reagent	Final concentration	Amount
BODIPY-C11 stock solution (5 mM)	5 μM	1 μL
Phosphate buffer saline (PBS, pH 7.4)	n/a	1 mL
Total	**5 μM**	**1 mL**

⚠ CRITICAL: Keep the working solution at room temperature (22 ± 2°C) for use and shielded from light. The maximum storage time is one month.

Note: For live cell imaging using PALP, complete cell culture medium is used to dilute the BODIPY-C11 working solution; for tissue analysis, both phosphate buffer saline (PBS, pH 7.4) and complete cell culture medium can be used to dilute the BODIPY-C11 stock solution.

KEY RESOURCES TABLE

REAGENT or RESOURCE	SOURCE	IDENTIFIER
Chemicals, peptides, and recombinant proteins		
BODIPY-C11	Life Technologies	Cat# D3861
ferrostatin-1	Cayman Chemical	Item No. 17729
liproxstatin-1	Cayman Chemical	Item No. 17730
deferoxamine	Cayman Chemical	Item No. 14595
DMSO	Sigma-Aldrich	Cat# D2650
penicillin/streptomycin	Gibco	Cat# 15140-122
fetal bovine serum	Gibco	Cat# 10270-106
phosphate buffer saline	Gibco	Cat# C10010500BT
Experimental models: Cell lines		
Human clear-cell renal cell carcinoma cell: 786-O	ATCC	Cat# CRL-1932, RRID: CVCL_1051
Human clear-cell ovarian carcinoma cell: ES-2	ATCC	Cat# CRL-1978, RRID: CVCL_3509
Human ovarian cancer cell: OVCAR-8	NCI-DTP	Cat# OVCAR-8, RRID: CVCL_1629
Human ovarian cancer cell: OV56	ECACC	Cat# 96020759, RRID: CVCL_2673
Human ovarian cancer cell: SKOV3	NICR	Resource# 4201PAT-CCTCC01017
Experimental models: Organisms/strains		
Mouse: athymic nude mice	The Jackson Laboratory	Strain# 007850
Software and algorithms		
Metamorph software	Molecular Devices, Andor	
ZEN 3.3 blue edition	Zeiss Microscope	https://www.zeiss.com/microscopy/int/products/microscope-software/zen.html
Nikon NIS Elements software	Nikon NIS Microscope	https://www.microscope.healthcare.nikon.com/products/software/nis-elements/viewer
ImageJ 1.52P	Fiji	https://imagej.net/software/fiji/
GraphPad Prism 9.0	GraphPad software Inc	https://www.graphpad.com/scientific-software/prism/
Adobe Illustrator	Adobe	www.adobe.com
Other		
RPMI 1640	Gibco	Cat# C11875500BT
DMEM	Gibco	Cat# C11995500BT
Low-Profile Disposable Blades 819	Leica Biosystems	Cat# LE63065-LP
Cryostat	Leica Biosystems	Cat# CM1950
Microscope slide, pathological grade	CITOTEST	Cat# 10127105P-G
Microscope cover slide	CITOTEST	Cat# 10212020C
A1R HD25 confocal microscope system	Nikon	N/A
LSM 800 confocal microscope system with Airyscan	Zeiss	N/A
LSM 880 confocal multiphoton microscope with Airyscan	Zeiss	N/A

STEP-BY-STEP METHOD DETAILS

Collecting and snap-freezing of tissue samples

Timing: 2–3 h

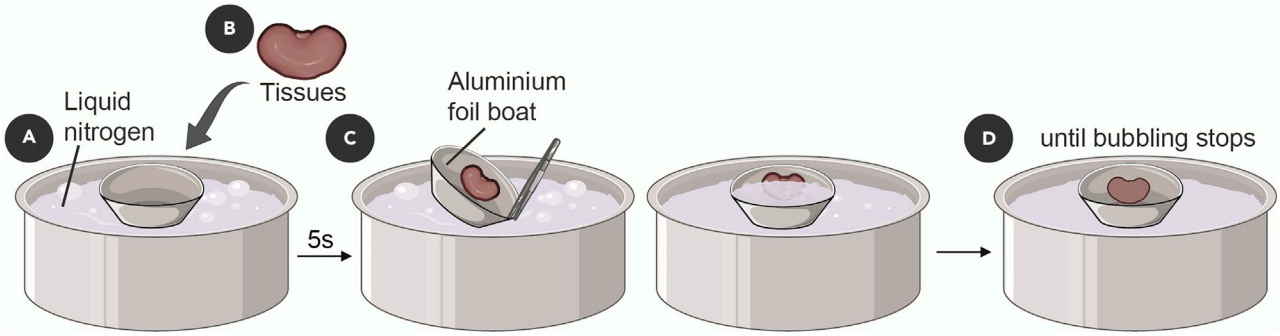

Figure 2. Schematic for snap-freezing tissues in liquid nitrogen, related to step 3

Before PALP analysis, tissue samples are dissected and flash-frozen in liquid nitrogen. Liquid nitrogen and washing buffer (deionized water) are prepared prior to the experiment. In this protocol, we used subcutaneous tumors isolated from 5-week-old female athymic nude mice as described above. However, tissues of interest from different age range and sex can be analyzed by the PALP technique.

1. Euthanize the mouse and dissect the tissue of interest for analysis.

   Note: We recommend using cervical dislocation for euthanizing the mouse to minimize perturbations on the metabolic characteristics of the tissue samples (Underwood and Anthony, 2020).

   Note: The PALP technique is applicable for analyzing various tissues including brain, kidney, heart, liver, spleen, and muscle.

2. Rinse the tissue samples briefly with deionized water to remove blood remnants.
3. Snap-freeze the tissue in liquid nitrogen. (See Figure 2)
   a. Fold a piece of aluminum foil into a boat shape and float on liquid nitrogen.
   b. Place tissue inside the foil boat.
   c. After 5 s, use forceps to gently press the foil boat and allow a small volume of liquid nitrogen to flow into the boat. Repeat until the tissue is completely submerged in liquid nitrogen.
   d. After evaporation of liquid nitrogen covering the tissue sample, remove tissue and wrap with aluminum foil.
   e. Frozen tissue can be stored at −80°C until use.

   Note: To preserve the membrane structure, tissue samples are best snap-frozen without optimal cutting temperature (OCT) as embedding material. To embed fragile or thin tissues such as skin, testis, and ovary, gelatin or 2.5% carboxymethylcellulose (CMC) are recommended as embedding medium (Nelson et al., 2013).

   Pause point: Frozen tissue samples can be kept in −80°C for long-term storage prior to tissue sectioning while avoiding freeze-thaw cycle. The maximum storage time for the frozen tissue samples is one year.

Cryosectioning of tissues

Timing: 2–3 h

The following steps prepare tissue sections for staining with BODIPY-C11 and PALP imaging.

4. Transfer the frozen tissue to −20°C at least 30 min prior to sectioning to equilibrate the temperature of the tissue to that inside the cryostat chamber.
5. Transfer the tissue to the cryostat chamber and affix the tissue to the specimen disc using ultrapure water.
6. Set the optimal cutting temperature. For tissues that contain higher fat deposition, slightly lower temperature for the cryostat is recommended. The cutting temperature is typically −20 ± 3°C, e.g., −18°C for kidney and −20°C for brain tissues.
7. Section the tissue to 10 μm (5–15 μm) and thaw mount sections onto glass slides.

Note: The thickness of the sections can be adjusted according to the tissue structures and applications. To ensure stable performance of the cryostat, the temperature should be strictly controlled throughout the sectioning process.

Pause point: Mounted tissue section slides can be kept at −80°C for long-term storage without freeze-thaw cycles and exposure to light.

⚠ CRITICAL: During the cryostat process, the tissues should be kept frozen to minimize metabolic changes and the sections should be kept hydrated to facilitate BODIPY-C11 staining.

Pre-staining of tissue sections with BODIPY-C11

Timing: 40 min

Even distribution of the BODIPY-C11 dye on the cellular membranes of tissue sections is critical for the success of PALP. The confocal system should be tuned for imaging at this stage. For live-cell imaging, users can start their experiment from this step.

8. Equilibrate the tissue section slide to room temperature (22 ± 2°C), then add 100 μL BODIPY 581/591 C11 working solution (1×) onto each slide and carefully cover the samples with coverslips.

Optional: Use brush to gently apply nail polish onto the edge of the coverslip to fix the coverslip.

Optional: For live-cell imaging, replace the culture medium supernatant with an appropriate amount of the BODIPY 581/591 C11 working solution (1×) prepared with culture medium.

9. Incubate the tissue section or cells with BODIPY-C11 for 30 min.

⚠ CRITICAL: Keep the section at room temperature during the pre-staining process, and incubate live cells undergoing staining in a cell culture incubator set at 37°C with 5% CO_2. Protect all samples from strong light exposure after BODIPY-C11 addition.

PALPv1: inducing lipid peroxidation and assess ferroptosis sensitivity in live cells or in tissue

Timing: 1 h

This section describes how to perform photochemical activation of membrane lipid peroxidation in tissues *in situ* or in live cells using a confocal microscope system (PALP version 1, PALPv1). PALPv1 using regular high-power lasers can presumably penetrate all membranes distributed along the z-axis of the analyzed sample.

10. Transfer the BODIPY-C11 conjugated tissue slides to the microscope stage and adjust the focal plane.

Note: The magnification of the objective lens is recommended at 60× to obtain high spatial resolution. This magnification can be adjusted based on the user's preferences.

11. Adjust the intensity of 488 nm and 561 nm laser scanning sources and detector voltage to avoid overexposure. Capture fluorescent signals of 488 nm (FITC) and 561 nm (TRITC) channels when they are stable. (Troubleshooting 1 and 3)

⚠ CRITICAL: Fluorescence from the reduced and oxidized BODIPY-C11 will be captured via the 488 nm (FITC) and 561 nm (TRITC) channels, respectively.

12. Select a small region of interest of around 2–4 μm^2. (Troubleshooting 2)

Note: The stimulated region is set at this parameter to focus the energy from the laser to enable lipid peroxidation induction.

13. Utilize the 405 nm high pulse laser from the confocal microscope light source to stimulate the selected region for 5 repeats of 200-ms interval.

Note: The stimulation parameter is applicable to live cell and tissue samples using Nikon A1R confocal microscope and Nikon spinning disk confocal microscope.

⚠ CRITICAL: For other fluorescent microscope models, adjust the laser parameters accordingly to induce optimal lipid peroxidation signal. Lasers that are of too weak intensity will not induce lipid peroxidation, whereas too strong lasers can quench the fluorescent dye or kill the cells.

14. Immediately acquire images from the 488 nm (FITC) and 561 nm (TRITC) channels. (Troubleshooting 4 and 5)

⚠ CRITICAL: The fluorescence signal in the targeted area is usually the strongest immediately after photochemical activation of lipid peroxidation. For quantification purposes, we recommend capturing and quantifying the fluorescence signals with no delay after applying laser stimulations.

PALPv2: inducing lipid peroxidation on a selected membrane along the z-axis in cells

Timing: 1 h

This section describes how to induce lipid peroxidation on selected membranes along the cellular z-axis using two-photon excitation microscopes (PALP version 2, PALPv2).

15. Place the glass chamber containing BODIPY-C11 pre-stained cells on the microscope stage and adjust the focal plane.

Note: For the Zeiss 880 multi-photon microscope, we recommend using 60× objective lens for live cell imaging; however, the users can adjust the magnification for different applications.

16. Adjust the intensity of 488 nm and 561 nm laser scanning sources and detector voltage to avoid overexposure. Acquire the pre-laser stimulation fluorescent signals from the 488 nm (FITC) and 561 nm (TRITC) channels. (Troubleshooting 1 and 3)

17. Select a defined region of interest around 2–4 μm^2.
18. Use multiple 800 nm low-energy photons to excite the same target molecule on the focal plane and induce lipid peroxidation. The laser power output and stimulation time for each microscope model should be adjusted to enable lipid peroxidation induction while avoiding quenching the BODIPY-C11 dye.
19. For image acquisition, immediately acquire fluorescent signals from the 488 nm (FITC) and 561 nm (TRITC) channels. We recommend acquiring the images at 0.4–0.6 μm intervals along the z-axis but this parameter can be adjusted. (Troubleshooting 4 and 5)

Data analysis: quantify PALP signals on regions of interest

Timing: 1 h

20. Analyze the fluorescent signal of the stimulated region using image processing softwares.
    a. Import the region of interest (ROI) to locate laser bleaching regions.
    b. Analyze the gray intensity of pre-PALP 488 nm (Ox_{pre}), pre-PALP 561 nm (Re_{pre}), and post-PALP 488 nm (Ox_{post}) channels.

Note: Post-PALP 561 nm (Re_{post}) channel signal is often lost or very weak due to oxidation of the BODIPY-C11 dye in an lipid hydroperoxide-rich environment after applying high-power lasers to focused regions, hence this signal is not used for normalizing PALP fluorescent signals.

⚠ CRITICAL: Images were acquired by Metamorph software for Andor confocal microscope, Nikon NIS Elements software for Nikon microscope, and ZEN blue edition for Zeiss microscope. Downstream image analysis can be performed using Fiji ImageJ.

21. We recommend using the following parameters to normalize and present the lipid peroxidation signals induced by laser stimulation across different samples:
    a. Ox_{post} / Re_{pre}, i.e., the oxidized BODIPY-C11 intensity post-stimulation divided by the reduced BODIPY-C11 fluorescence pre-stimulation.
    b. (Ox_{post} - Ox_{pre}) / Re_{pre}, i.e., the difference between the oxidized BODIPY-C11 intensity post-stimulation versus pre-stimulation, and this is divided by the reduced BODIPY-C11 fluorescence pre-stimulation.

Note: To normalize the absorption and integration of BODIPY-C11 with samples, **"a"** method is recommended. To exclude the pre-PALP background signals of oxidative lipids, **"b"** method is adopted.

⚠ CRITICAL: We recommend sampling multiple regions of the same tissue to obtain a comprehensive assessment of the spatial distribution of the ferroptosis sensitivity on the sample.

EXPECTED OUTCOMES

By following this protocol, users can expect to track lipid peroxidation dynamics, assess polyunsaturated phospholipid levels, and stratify ferroptosis sensitivity of live cells and tissues. PALP stimulation can induce strong oxidative BODIPY-C11 signals in ferroptosis-susceptible samples.

For live-cell imaging, we pretreated ferroptosis-susceptible 786-O clear-cell renal cell carcinoma cells and ES-2 clear-cell ovarian carcinoma cells with iron chelator deferoxamine (DFO), or lipophilic radical-trapping antioxidants ferrostatin-1 (Fer-1) and liproxstatin-1 (Lip-1) (Dixon et al., 2012; Friedmann Angeli et al., 2014; Zilka et al., 2017). The final concentration of DFO, Fer-1, and Lip-1 in the assays was 50 μM, 5 μM, and 1 μM, respectively. 4-h treatment with each of the three chemicals prior

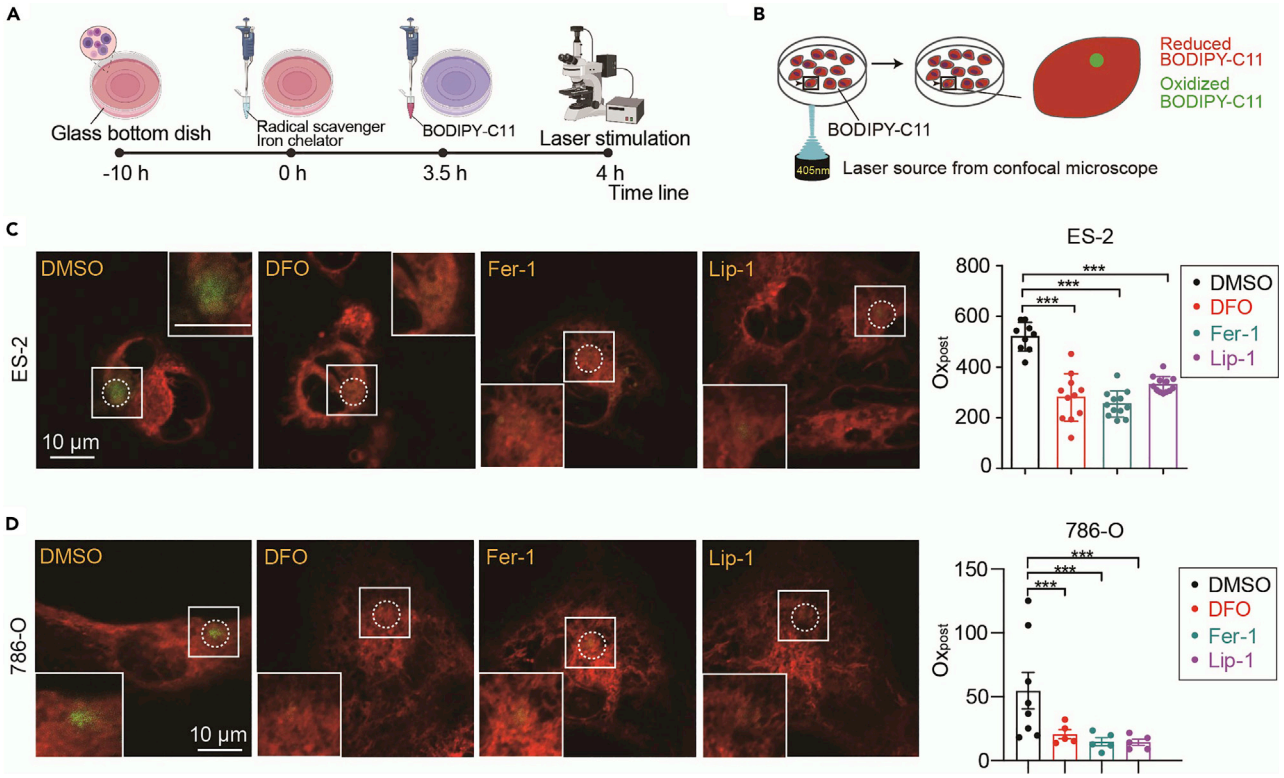

Figure 3. PALPv1-induced fluorescence in live cells, related to expected outcomes

(A) Graphical schematic summarizing the experimental procedure in (C and D). Briefly, DMSO, Fer-1 (5 μM), Lip-1 (1 μM) or DFO (50 μM) were added 4 h prior to laser stimulation, whereas BODIPY-C11 was added 30 min prior to stimulation.

(B) Schematic describing the procedures of the photochemical activation of membrane lipid peroxidation (PALPv1) technique.

(C and D) Representative fluorescent images showing the PALP-induced fluorescence post application of 405 nm laser pulses to ES-2 (C) and 786-O (D) cells treated with DMSO, Fer-1, Lip-1 or DFO. Green, oxidized BODIPY-C11 signal; red, reduced BODIPY-C11 signal. On the right, quantifications of the PALP-induced fluorescence intensities of analyzed regions. The dotted circles represent the regions where the laser was applied. The number of cells analyzed in each experiment are indicated by the plots. Lines and error bars indicate mean ± s.d. Statistical analysis was performed using two-tailed, unpaired student's T-test. ***, $p < 0.001$. Representative results from three independent experiments. Scale bar indicates 10 μm. This figure was reused from Wang et al. (2021).

See also Methods video S1.

to PALP stimulation significantly suppressed the signal of PALPv1-induced fluorescence in both ES-2 and 786-O cells (Figure 3, Methods video S1).

To assess ferroptosis sensitivity of tumor tissues *in situ*, we subcutaneously implanted immunocompromised mice with four ovarian cancer cell lines that exhibit different ferroptosis sensitivities, with the sensitivity rank of ES-2 > OVCAR-8 > OV56 > SKOV3 (Wang et al., 2021). We applied high-power laser to randomly selected, localized regions (n=16 ± 4) in xenograft sections representative of the tumor tissue's sensitivity to ferroptosis. The PALPv1 signal ranking of ovarian xenograft tumor sections was also ES-2 > OVCAR-8 > OV56 > SKOV3 (Figure 4).

To track lipid peroxidation dynamics on selected membranes along the z-axis in live cells, we applied PALPv2 to 786-O cells and only the areas near the focal plane along the z-axis exhibit strong oxidative BODIPY-C11 signals (Figure 5, Methods video S2).

LIMITATIONS

We use a high-power laser to induce lipid peroxidation in membranes. To focus the energy from the laser for efficient lipid peroxidation induction without causing cell death, PALP stimulation is

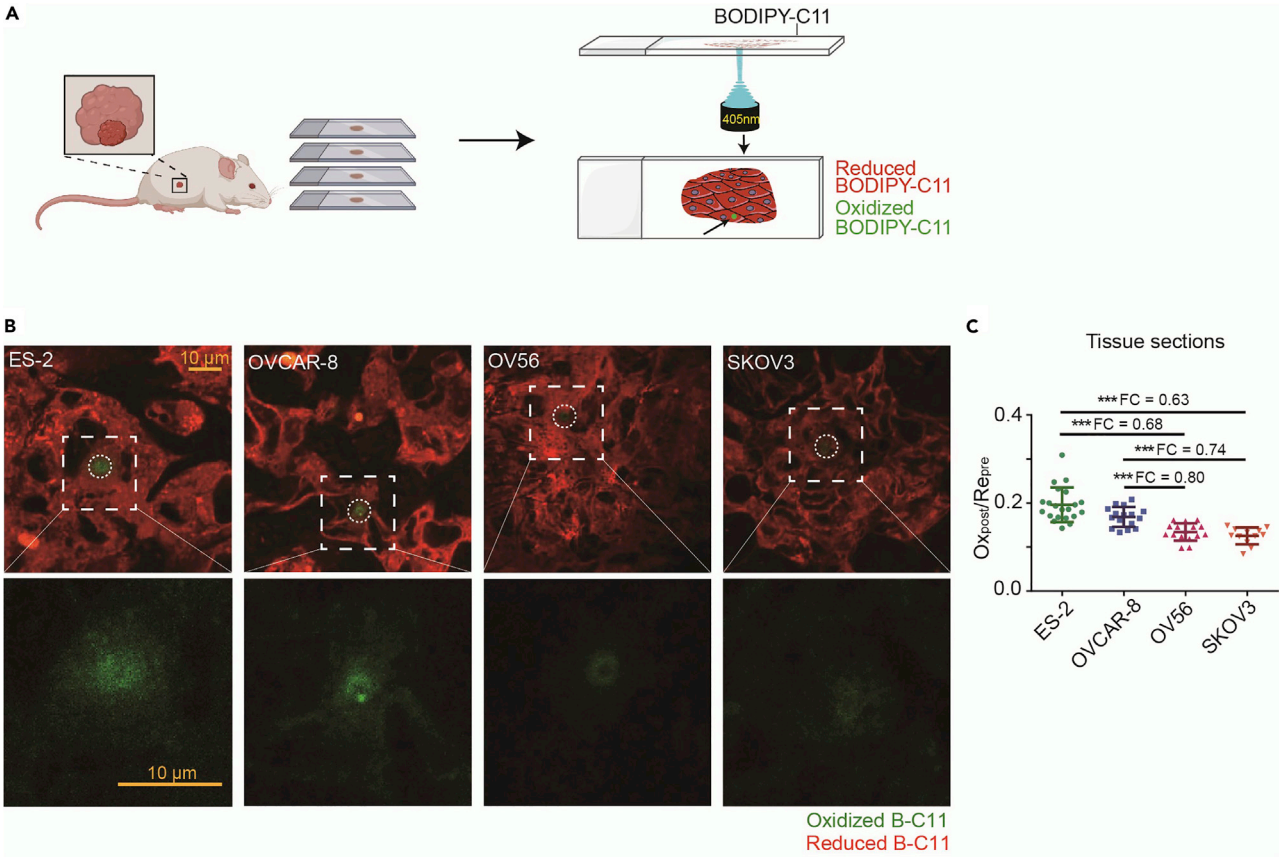

Figure 4. PALPv1-induced fluorescence in human ovarian xenograft tumors *in situ*, related to expected outcomes

(A) Graphical schematic describing the procedures of PALPv1 technique for tissue sections, related to steps 10–14.

(B) Representative fluorescent images showing the PALP-induced fluorescence post-application of laser pulses to xenograft tumor sections including human ovarian ES-2, OVCAR-8, OV56, and SKOV3 cells. Green, oxidized BODIPY-C11 signal; red, reduced BODIPY-C11 signal. Scale bar indicates 10 μm.

(C) Scatter plots showing the Ox_{post} / Re_{pre} BODIPY-C11 fluorescence of PALP signals in xenograft tumor sections including human ovarian ES-2, OVCAR-8, OV56, and SKOV3 cells. Dots and error bars, mean ± s.d. Two-tailed unpaired T-test, ***, $p < 0.001$. FC, fold-change. This figure was reused from Wang et al. (2021).

restricted to a small region that is less than 10 μm^2. Hence, our protocol for stratifying ferroptosis sensitivity is limited in spatial throughput, and multiple regions need to be sampled to achieve a comprehensive evaluation of the ferroptosis sensitivity on a prepared tissue sample. Secondly, the lipid peroxidation dye BODIPY-C11 has different penetration efficiency in various cell types and tissues. For different cell lines, users are suggested to compare the PALP-induced signal intensity by normalizing the oxidative BODIPY-C11 fluorescent signal post-stimulation to reduced pre-stimulation BODIPY-C11 signal (Ox_{post} / Re_{pre}). Thirdly, different models of high-power laser sources have different power outputs and varying lipid peroxidation induction efficacy, hence, PALP induced signal from different microscope systems is not necessarily directly comparable. In addition, the PALP technique in its current form is compatible with live cell marker staining, providing information on the specific cell types targeted before PALP analysis. However, the fluorescent signal of cellular markers may be quenched after applying a high power laser.

TROUBLESHOOTING

Problem 1

Both reduced and oxidative BODIPY-C11 signals from different cells vary significantly, the background signal affects PALP-induced fluorescence (steps 11 and 16)

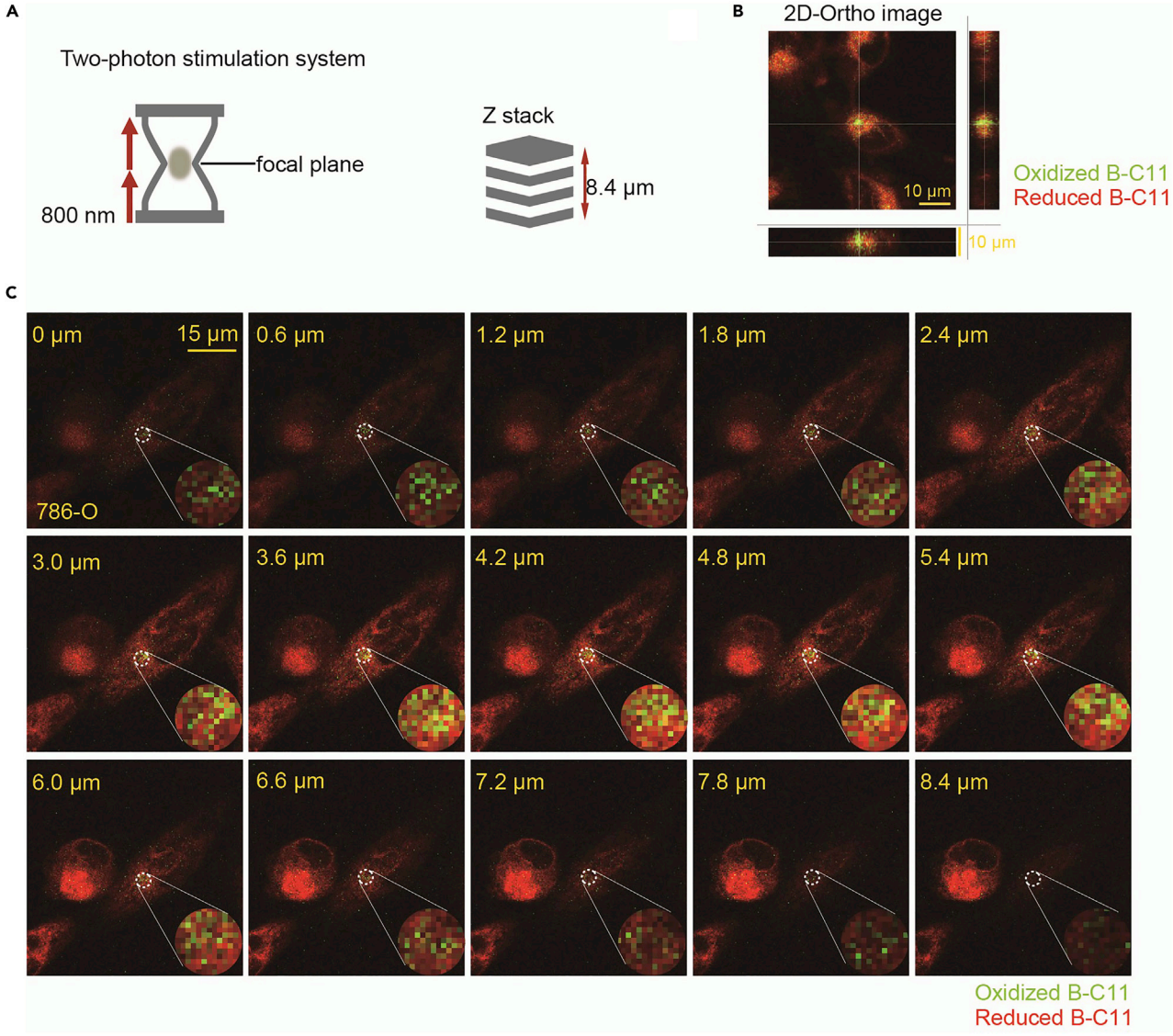

Figure 5. PALPv2 improves the z-axis resolution using laser sources from two-photon confocal microscopes, related to expected outcomes

(A) Schematic diagram of two-photon excitation confocal microscope system. The focal plane was stimulated by two 800 nm infrared photon beams, while the non-focal-plane could not be excited. Every 0.6 μm thickness of the cell was captured along the z-stack.

(B) Representative 2-D orthogonal image of 786-O cells stimulated by PALPv2. Scale bar indicates 10 μm. Green, oxidized BODIPY-C11 signal; red, reduced BODIPY-C11 signal.

(C) Representative fluorescent images showing the Z-stack series of the reduced and oxidized BODIPY-C11 signal after the application of 100% 800 nm two-photon excitation in 786-O cells. Scale bar indicates 15 μm. Green, oxidized BODIPY-C11 signal; red, reduced BODIPY-C11 signal. This figure was reused from Wang et al. (2021).

See also Methods video S2.

Potential solution

BODIPY-C11 is a lipophilic dye that associates with membranes. Different types of cells exhibit different lipid content and variable BODIPY-C11 dye penetration efficiency. Hence, there will be variations in the signal from reduced BODIPY-C11 (561 nm) prior to PALP induction. To assess the ferroptosis sensitivity of cells, we recommend using the ratio between oxidized and reduced BODIPY-C11 (Ox_{post} / Re_{pre}), rather than the oxidized BODIPY-C11 signal (Ox_{post}) alone. Consider subtracting the basal level of BODIPY-C11 oxidation (Ox_{pre}) when this signal is substantial.

Problem 2

Occasionally, when the laser is targeted to cellular regions with low BODIPY-C11 (Re_{pre}) distribution, PALP will not induce oxidized BODIPY-C11 signal in the 488 nm channel (step 12).

Potential solution

One limitation of the PALP technique is that it can only assess the polyunsaturated lipid level and relative ferroptosis sensitivity in cellular structures that the BODIPY-C11 dye can effectively penetrate and stain, for example, the endoplasmic reticulum. We recommend using the images of the pre-laser BODIPY-C11 (Re_{pre}) distribution to guide the selection of PALP regions to be targeted by the laser. For live cells, cellular structures (e.g., the endoplasmic reticulum and mitochondria) that exhibit strong BODIPY-C11 pre-staining are suitable candidate regions for PALP analyses.

Problem 3

The reduced BODIPY-C11 signal before PALP application is weak or quenched (steps 11 and 16).

Potential solution

One possible reason to this problem is that the BODIPY-C11 solution is degraded or inactivated due to light exposure. Users need to keep the staining solutions shielded from light throughout the pre-staining and PALP application process. Another plausible reason is that the solution lost its quality after multiple freeze-thaw cycles. We recommend aliquoting the stock solution to small volumes to avoid freeze-thaw cycles.

Problem 4

After applying PALP laser to a region with high Re_{pre} signal, the oxidative BODIPY-C11 signal does not increase (steps 14 and 19).

Potential solution

Please check the settings of the laser associated with the microscope to ensure sufficient power can be triggered and targeted to a focused sample area (<10 μm^2). If the laser settings are correct, the low signal of oxidative BODIPY-C11 represents that the tissue is potentially resistant to lipid peroxidation and ferroptosis induction.

Problem 5

The oxidative BODIPY-C11 fluorescent signal diffuses rapidly after applying laser to the region of interest (steps 14 and 19).

Potential solution

Lipid peroxidation could be triggered by PALP in highly mobile or dynamic cellular structures such as the endoplasmic reticulum or intracellular vesicles. In these cases, the oxidized BODIPY-C11 molecules may be carried to other cellular spaces rapidly along with the targeted cellular structure. These are intrinsic features of cells undergoing targeted lipid peroxidation and can be potentially investigated accordingly.

RESOURCE AVAILABILITY

Lead contact

Further information and requests for resources and reagents should be directed to and will be fulfilled by the lead contact, Yilong Zou (zouyilong@westlake.edu.cn).

Materials availability

This study did not generate new unique reagents.

Data and code availability

Raw videos showing the dynamics of BODIPY-C11 fluorescence in live cells are provided as multiple Methods video S1 and S2. These data are publicly available as of the date of publication.
This paper does not report original code.
Any additional information required to reanalyze the data reported in this paper is available from the lead contact upon request.

SUPPLEMENTAL INFORMATION

Supplemental information can be found online at https://doi.org/10.1016/j.xpro.2022.101189.

ACKNOWLEDGEMENTS

We thank members of the Zou lab for insightful discussions and the Westlake University Microscopic Imaging Platform for assisting the microscope training and usage. This work was supported by the Westlake Education Foundation and the Westlake Laboratory of Life Sciences and Biomedicine.

AUTHOR CONTRIBUTIONS

Conceptualization, Y.Z., F.W., and N.N; Writing – original draft, F.W. and N.N; Writing – review & editing, Y.Z., F.W., and N.N.; Funding Acquisition, Y.Z; Supervision, Y.Z.

DECLARATION OF INTERESTS

Y. Z. is a consultant at Keen Therapeutics. The remaining authors declare no competing interests. A patent describing the utility of PALP in clinical samples was filed by Y.Z., F.W., N.N., *et al.*

REFERENCES

Dixon, S.J., Lemberg, K.M., Lamprecht, M.R., Skouta, R., Zaitsev, E.M., Gleason, C.E., Patel, D.N., Bauer, A.J., Cantley, A.M., Yang, W.S., et al. (2012). Ferroptosis: an iron-dependent form of nonapoptotic cell death. Cell *149*, 1060–1072.

Drummen, G.P.C., van Liebergen, L.C.M., Op den Kamp, J.A.F., and Post, J.A. (2002). C11-BODIPY581/591, an oxidation-sensitive fluorescent lipid peroxidation probe: (micro)spectroscopic characterization and validation of methodology. Free Radic. Biol. Med. *33*, 473–490.

Friedmann Angeli, J.P., Schneider, M., Proneth, B., Tyurina, Y.Y., Tyurin, V.A., Hammond, V.J., Herbach, N., Aichler, M., Walch, A., Eggenhofer, E., et al. (2014). Inactivation of the ferroptosis regulator Gpx4 triggers acute renal failure in mice. Nat. Cell Biol. *16*, 1180–1191.

Jiang, X., Stockwell, B.R., and Conrad, M. (2021). Ferroptosis: mechanisms, biology and role in disease. Nat. Rev. Mol. Cell Biol. *22*, 266–282.

Nelson, K.A., Daniels, G.J., Fournie, J.W., and Hemmer, M.J. (2013). Optimization of whole-body zebrafish sectioning methods for mass spectrometry imaging. J. Biomol. Tech. *24*, 119–127.

Underwood, W., and Anthony, R. (2020). AVMA Guidelines for the Euthanasia of Animals: 2020 Edition, Retrieved on March 2013, 2020–2021.

Wang, F., Graham, E.T., Naowarojna, N., Shi, Z., Wang, Y., Xie, G., Zhou, L., Salmon, W., Jia, J.-M., Wang, X., et al. (2021). PALP: a rapid imaging technique for stratifying ferroptosis sensitivity in normal and tumor tissues in situ. Cell Chem. Biol. *29*, 157–170.e6.

Zilka, O., Shah, R., Li, B., Friedmann Angeli, J.P., Griesser, M., Conrad, M., and Pratt, D.A. (2017). On the mechanism of cytoprotection by ferrostatin-1 and liproxstatin-1 and the role of lipid peroxidation in ferroptotic cell death. ACS Cent. Sci. *3*, 232–243.